Atmospheric and Climate Sciences, 2025, 15(1), 175-186
https://www.scirp.org/journal/acs
ISSN Online: 2160-0422
ISSN Print: 2160-0414

Comprehensive Analysis of the Ionospheric Response to the 2015 Geomagnetic Storms over Different Station

Aidashisha Bareh, Bornali Chetia

Physics Department, The Assam Royal Global University, Guwahati, India
Email: aidabareh18@gmail.com

How to cite this paper: Bareh, A. and Chetia, B. (2025) Comprehensive Analysis of the Ionospheric Response to the 2015 Geomagnetic Storms over Different Station. *Atmospheric and Climate Sciences*, **15**, 175-186.
https://doi.org/10.4236/acs.2025.151008

Received: November 26, 2024
Accepted: January 13, 2025
Published: January 16, 2025

Abstract

The fundamental problem of ionospheric physics lies in understanding and modeling the ionosphere's dependence on solar activity. This challenge encompasses such as Variables across Solar Cycles, Response to Solar Flares and CMEs, Daily and Seasonal Effects, Spatial Variability and long term prediction models. This dependency on solar activity helps provide information that is fundamental to comprehend the changes in the ionosphere and its processes. In this work, the ionospheric critical frequency foF2 and electron density are applied to characterize large-scale ionosphere responses during the 2015 geomagnetic storm. Using data from the International Reference Ionosphere (IRI-2016 model), an empirical standard model of the Ionosphere, this work tries to construct a correspondence between the solar activity and the change in the Ionosphere's characteristics across three different stations at different altitudes. It has been observed that the electron density decreases from (1.098E + 12 to 7.844E + 11) for low latitude, (6.358E + 11 to 3.650E + 11.) for mid latitude and (4.765E + 11 to 2.740E + 11) for high latitude on the day of the solar event. A similar decrease in foF2 by 40% - 70% can also be seen for the three different stations on the geomagnetic storm day.

Keywords

Electron Density, foF2, Geomagnetic Storm, IRI 2016

1. Introduction

Geomagnetic storms are short-term disturbances caused by the solar wind that affect the Earth's magnetosphere. When the magnetic field of the solar wind interacts with the Earth's magnetic field, it initially compresses the Earth's magnetosphere. A solar flare is a brief eruption of intense energy and is associated with the release of magnetic energy stored in the solar atmosphere. In years of solar maximum, solar flares commonly occur. During solar flares, large amounts of energy are suddenly released from the Sun, causing an increase with different amplitudes, including the wavelength of radio waves, visible light, and XUV (extreme ultraviolet) radiation. After travelling at the speed of light for eight minutes, explosive radiation finally reaches Earth. The flares cause unexpected ionospheric disturbances by quickly altering the ionosphere's structure and state as well as that of the thermosphere in the hemisphere that receives sunlight. The disturbance phenomena encompass various issues, such as short-wave fadeouts, sudden phase anomalies, frequency disturbances, magnetic solar flare effects, and an elevation in Total Electron Content (TEC). These phenomena are caused by a sudden increase in the electron density in the D region, which also leads to impulsive cosmic noise absorption. Solar proton events occur when solar energetic particles, mainly protons are ejected from the sun during solar flare. In the hemisphere with sunlight, the solar energetic particles and X-ray effects are combined. The neutral atmosphere and ionosphere are substantially impacted by the particles released during these events, particularly in polar locations, which causes significant increases in the concentrations of HOx (H, OH, and HO_2) and NOx (N, NO, and NO_2) in the mesosphere and stratosphere. They reduce the ozone level even more. The polar D zone can be penetrated by SEPs, increasing the ionization rate there and enhancing radio wave absorption. The main sources of extreme solar ultraviolet emissions that contribute to the ionosphere are the Sun's chromosphere and corona, but these emissions are not coordinated. This is because the ionosphere is intricately influenced by chemical, dynamical, and electrodynamic processes, all of which are modulated by solar activity. The direct impact of XUV ionization and the broader response to solar variations also contribute to the dynamic behavior of the ionosphere, with chemical and dynamical processes exhibiting variation on different spatial scales.

The ionosphere comprises free electrons and positive ions, which are ionized components and are generally equal in number in a medium that is electrically neutral. The ionosphere lies about 48 km to 965 km above sea level. The ionosphere includes the thermosphere and some parts of the mesosphere and exosphere. The ionosphere is important due to its vital role in radio propagation to different places on Earth. Ionospheric studies utilize a range of observing techniques, such as ionosonde measurements which provide a vertical profile of electron density, trans-ionospheric radio signals that help analyze signal behavior through the ionosphere, and incoherent radar systems which offer insights into ionospheric dynamics [1]-[6]. Over the last decade, the extensive use of Global Positioning System (GPS) data has significantly contributed to ionospheric studies [7] [8].

Space weather encompasses various factors, such as solar wind, geomagnetic activity, solar ionizing radiation, and long-term changes in Earth's magnetic field. These elements contribute to the ionospheric climate, shaping the dynamic conditions in space that can impact communication, navigation, and other technologies reliant on interactions with Earth's atmosphere and magnetic field. However, during a geomagnetic storm, energy from the solar wind is transferred to Earth's magnetosphere. This energy transfer can lead to increased activity in the ionosphere and atmosphere, particularly at high and mid-latitudes [9] [10].

The critical frequency of the F2 region (foF2) plays a crucial role in ionospheric characterization. Geomagnetic storms can significantly impact the F2 region, and solar extreme ultraviolet (EUV) irradiances are key factors in ionization at medium and low latitudes. Establishing a connection between ionospheric features and solar activity is vital for empirical models. Climatological models successfully describe foF2 variations with respect to local time, season, and the solar cycle, aiding in understanding and predicting ionospheric behavior under different conditions [11]. In this paper, we report on a systematic survey of sudden electron density changes in the daytime ionosphere, and its exploration of potential connections with solar flares. Utilizing vertical profiles of electron density data from three different stations and leveraging the IRI-2016 model adds a robust dimension to the analysis. This approach allows for a comprehensive examination of how solar flares may influence electron density dynamics in the ionosphere during daytime conditions. Also critical frequency of F2 layer (foF2) data from different stations in Japan, such as Kokubunji, Okinawa, and Wakkanai is collected from SIDC for 2015 geomagnetic storm event.

2. Methodology

The Solar Cycle 24 had its maximum in the year 2015 and on the day of 23rd June, solar activities peaked. In order to find the impact of solar activities on the ionosphere, electron densities and foF2 data are collected around that day across three different stations, Okinawa (26.21˚N, 127.68˚E), Kokubunji (35.71˚N, 139.46˚E) and Wakkanai (45.41˚N, 141.67˚E).

Electron density data have been collected from International Reference Ionosphere (IRI). The International Reference Ionosphere (IRI-2016) model, a global effort supported by organizations like the International Union of Radio Science and the Committee on Space Research (COSPAR), highlights the collaborative nature of ionospheric research. The establishment of a working group in the late 1960s, tasked with creating an empirical standard model based on all available data sources, underscores the importance of such standardized models. Our study relies on hourly values of foF2, obtained from the Space Physics Data Facility (SPDF) of NASA Goddard Space Flight Center through the Omniweb data explorer service. Additionally, the use of hourly averaged values from Syowa station in Antarctica, provided by the National Institute of Information and Communications Technology (NICT), Japan (http://wdc.nict.go.jp/IONO/HP2009/ISDJ/index-E.html), adds a specific and valuable dataset to our analysis. This multi-source approach enhances the robustness of our study's findings.

Several geomagnetic storms occurred in 2015, including both moderate and severe events. Among them, two severe geomagnetic storms, on 17th March 2015 and 23rd June 2015, reached a Dst (Disturbance Storm Time index) intensity of −200nT. As both events exhibited similar effects, this paper focuses on the geomagnetic storm of 23rd June 2015.

Here, we considered five days prior to the day of the event and five days after, *i.e.* from 18 June to 28 June. Thus, for a total of 11 days, we noted down the hourly variation of the ionosphere's electron density, for each of the three stations. In this paper, a specific approach has been adopted to identify fluctuations in electron density, NmF2 and critical frequency, foF2 during geomagnetic storms, distinguishing them from the normal quiet-day patterns of NmF2 and foF2. First, the 10 quietest days of the month were selected, and hourly averages were computed for each day. Additionally, the standard deviation for these quiet days was calculated hourly using the following formula

$$\sigma = \sqrt{\frac{1}{N}\sum_{i=1}^{N}\left(x_i - x'\right)^2}$$

where σ = standard deviation, x_i = each data point in the dataset, x' = average mean and N = Total number of data points.

These data were then plotted in contour graphs for each of the station. It is possible to display a three-dimensional surface on a two-dimensional plane using contour plots, also known as level plots. It plots a response variable Z as contours together with two predictor variables X and Y on the y-axis. These graphs will help us visualize the correlation between the altitudes, latitudes and days.

3. Result

On 23rd June 2015, a severe geomagnetic storm with intensity of Dst −200nT took place as shown in **Figure 1** and it has an impact on various parameters like electron density NmF2 and critical frequency foF2. The intensity of the storm also has an effect on other solar activity indicators, such as the Kp-index (as shown in **Figure 2**), Ap-index, and sunspot number, causing changes in their values. The ionospheric response to these impacts is different for different stations depending on their latitudes.

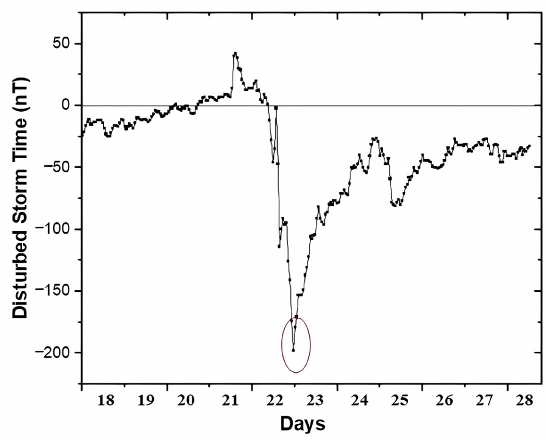

Figure 1. Disturbed storm time (Dst index) profile for 23rd June 2015.

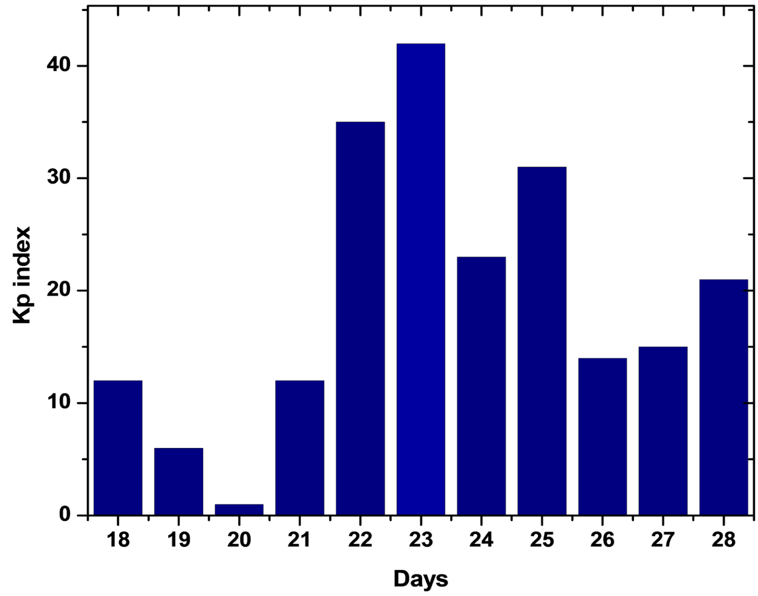

Figure 2. Kp index profile for 23rd June 2015.

Figure 3 is drawn against electron density for the month of June 2015 for Okinawa Station (26.21 N, 127.68 E). Here, 11 days (5 days before and 5 days after the event) has been considered for the study with altitude from 200 km to 400 km. It is seen from the profile that the electron density is maximum at 290 - 380 km. It has also been observed that on the day of the solar event *i.e.*, on 23rd June 2015, the electron density decreases to about 7.844E + 11 from 1.098E + 12.

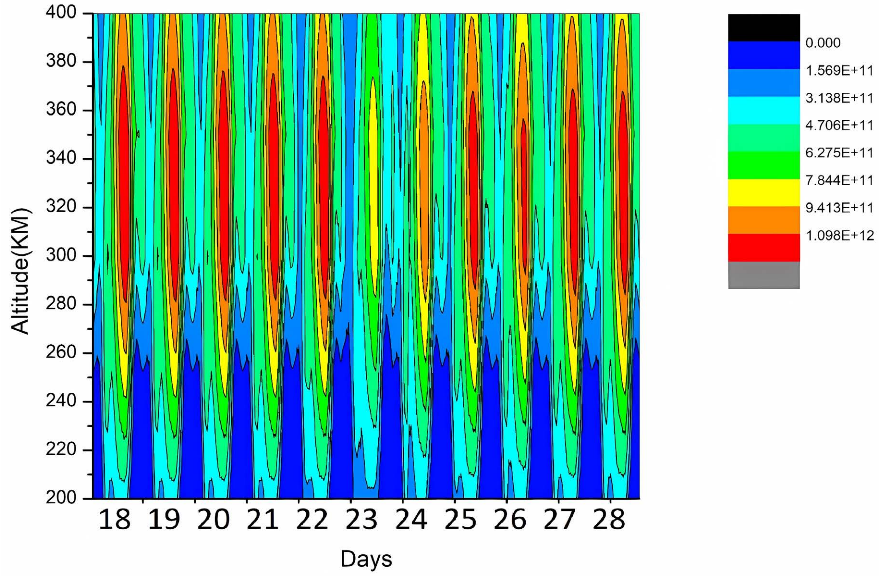

Figure 3. Electron density profile for Okinawa station (26.21°N, 127.68°E) from 18 June to 28 June 2015, with the altitude ranging from 200 km to 400 km.

Similar study is carried out for Kokubunji Station (35.71°N, 139.46°E) which is depicted in Figure 4 for the month of June 2015. Here, 11 days (5 days prior to the occurrence and 5 days following it) with an altitude ranging from 200 km to 400 km have been taken into account for the study. The plot shows that the electron density reaches its highest between 270 - 350 km. Additionally, it has been noted that on the day of the solar event, or on June 23, 2015, the electron density drops from 6.358E + 11 to around 3.650E + 11.

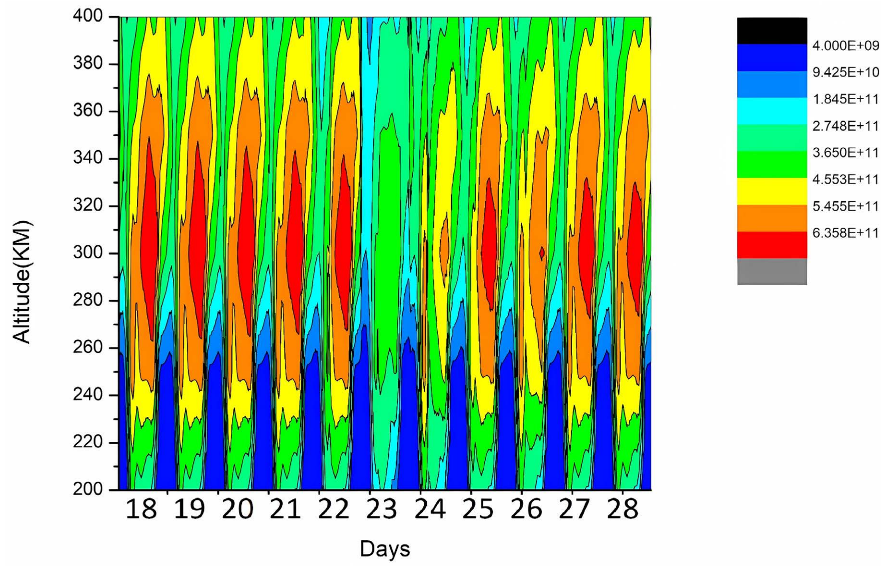

Figure 4. Electron density profile for Kokubunji Station (35.71°N, 139.46°E) from 18 June to 28 June 2015, with the altitude ranging from 200 km to 400 km.

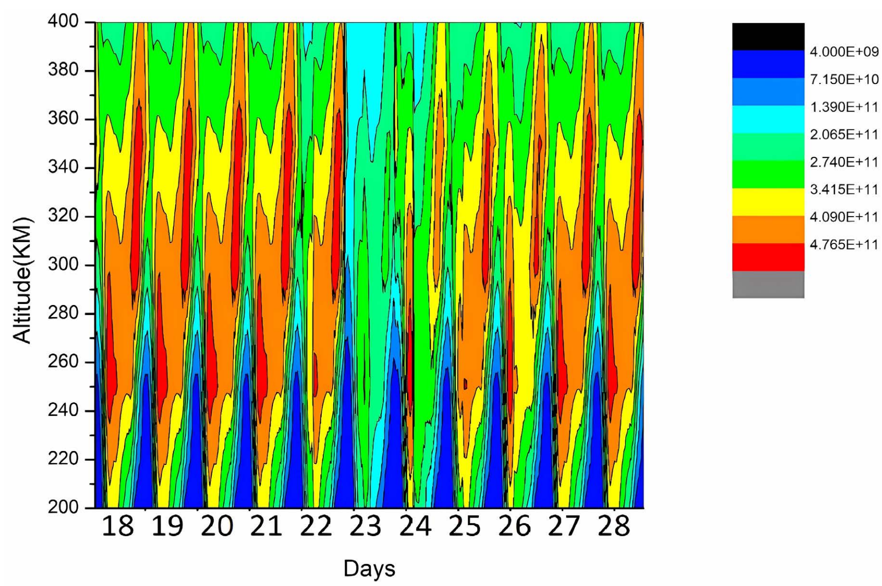

Figure 5. Electron density profile for Wakkanai Station (45.41°N, 141.67°E) from 18 June to 28 June 2015, with the altitude ranging from 200 km to 400 km.

Figure 5 displays the electron density profile for different altitudes for the month of June 2015 over Wakkanai Station (45.41°N, 141.67°E). For this study, 11 days with an altitude ranging from 200 km to 400 km have been included (5 days prior to the occurrence and 5 days after it). The plot demonstrates that between, 240-360 km the electron density is at its maximum. Additionally, it has been observed that the electron density decreases from 4.765E + 11 to roughly 2.740E + 11 on the day of the solar event, or on June 23, 2015.

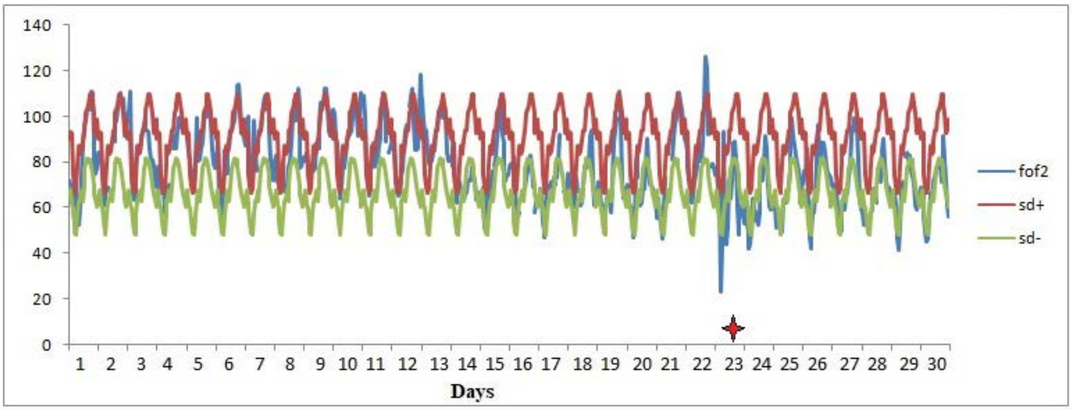

(a)

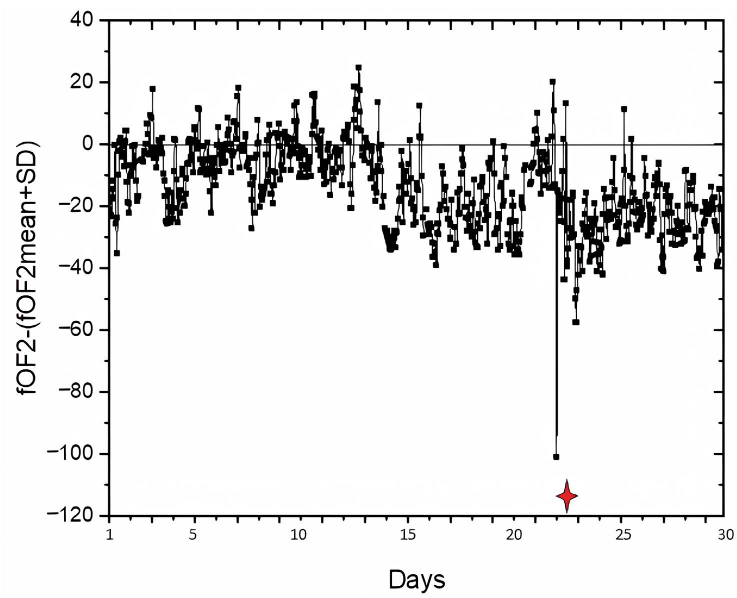

(b)

Figure 6. (a) Daily variation of foF2 (MHz) during June 2015 magnetic storm over Okinawa (26.2124˚N, 127.6809˚E) (b) SD (average) plot of foF2 during June 2015 magnetic storm over Okinawa (26.2124˚N, 127.6809˚E).

A typical foF2 profile during the geomagnetic storm event of June 23, 2015, is presented in Figure 6(a) & Figure 6(b). A change in foF2 on event day as well as quiet mean variation with standard deviation is shown in Figure 6(a) and a percentage deviation due to solar storm is given in Figure 6(b). Here, the decreasing trend in foF2 on the storm day by 100% indicates a substantial impact on plasma loss over Okinawa station with latitude (26.2124˚N, 127.6809˚E). Hence, compared to a normal day, the dominance of plasma loss over production rate on the event day suggests a significant impact on ionospheric behavior. Ionospheric observations during solar events become crucial in understanding transient properties, especially in relation to the changes in the magnetic field induced by solar wind. This information contributes significantly to our understanding of the complex dynamics in the ionosphere during such events.

Similar study has been carried out over Kokubunji station with latitude (35.7103˚N, 139.4632˚E). Figure 7(a) shows a variation in foF2 on event day as well as quiet mean variation and a percentage deviation due to solar storm is given in Figure 7(b). The analysis shows a decrease in foF2 up to 40% at the time of the event over Kokubunji station.

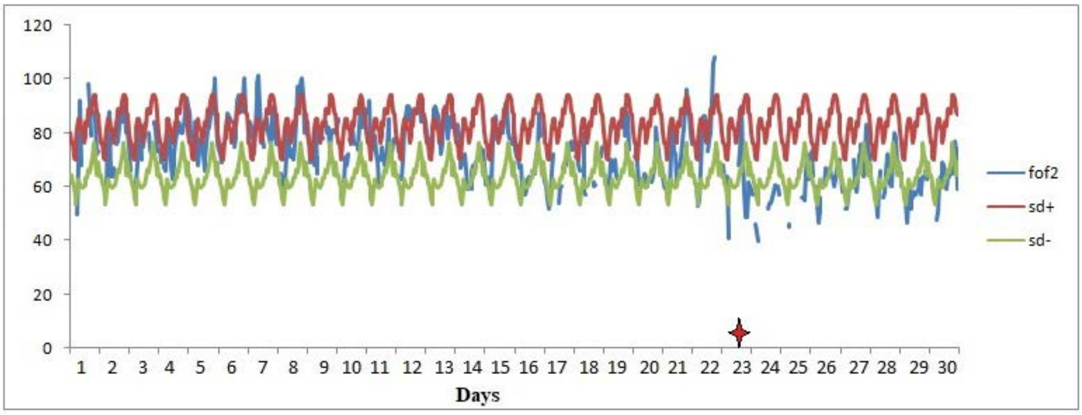

(a)

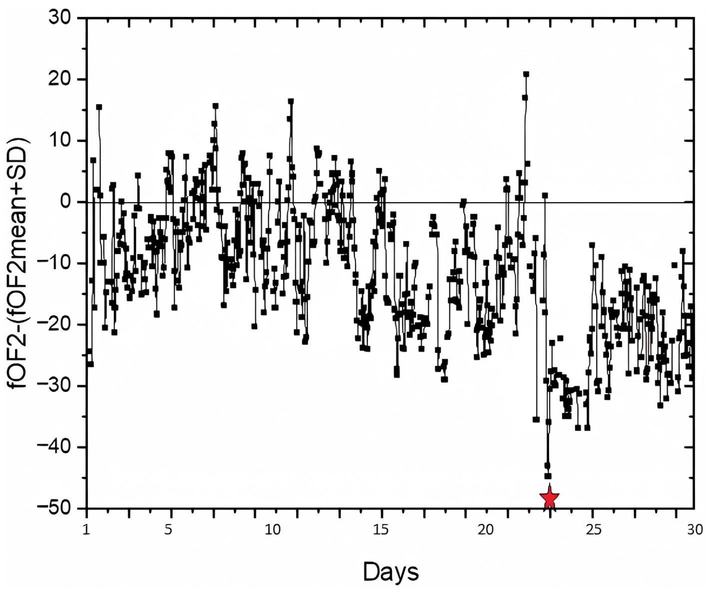

(b)

Figure 7. (a) Daily variation of foF2(MHz) during June 2015 magnetic storm over Kokubunji (35.7103˚N, 139.4632˚E) (b) SD (average) plot of foF2 during June 2015 magnetic storm over Kokubunji (35.7103˚N, 139.4632˚E).

Similarly in Figure 8(a) and Figure 8(b), a variation of foF2 has been carried out for 23rd June 2015 magnetic storm over Wakkanai station with latitude (45.4157˚N, 141.6731˚E). Here the figure also depicts a decreasing trend in foF2 with 70% from its normal SD limit.

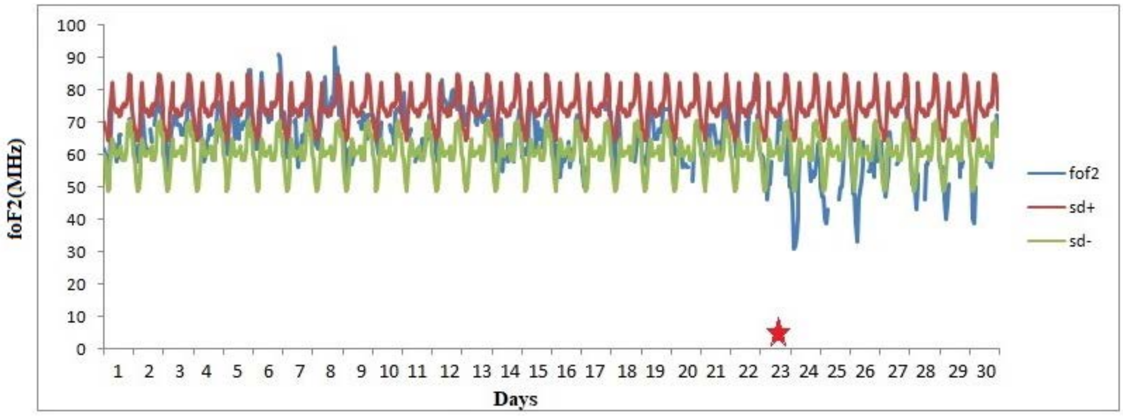

(a)

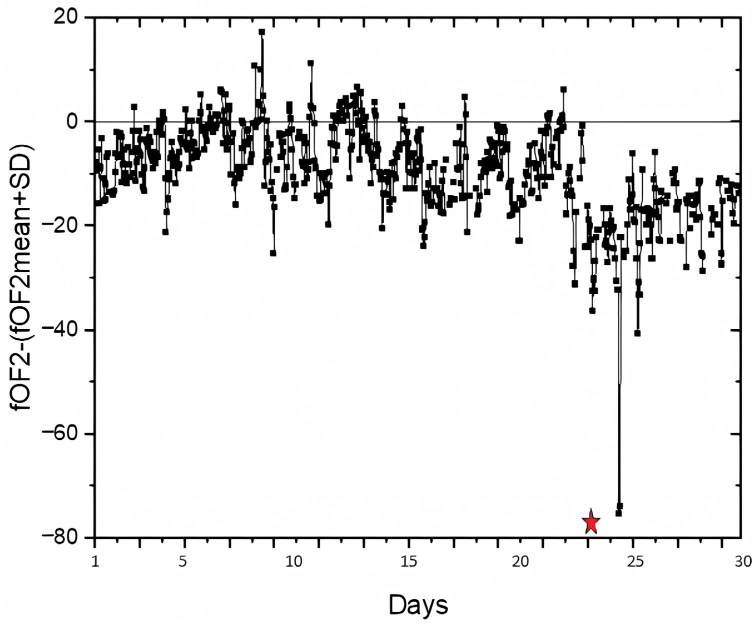

(b)

Figure 8. (a) Daily variation of foF2(MHz) during June 2015 magnetic storm over Wakkanai (45.4157˚N, 141.6731˚E) (b) SD (average) plot of foF2 during June 2015 magnetic storm over Wakkanai (45.4157˚N, 141.6731˚E).

Examining the foF2 anomalies observed by three different ionospheric stations during the June 2015 geomagnetic storm, our investigation focused on identifying instances of significant ionospheric perturbations. The two-phase storm effect, as observed in **Figure 7(b)**, often accompanies negative anomalies linked to enhanced auroral and geomagnetic activity. The positive phase in the foF2 trend is influenced by particle precipitation and Joule heating in the auroral regions, leading to pressure gradients and equatorial neutral winds. This, in turn, produces the negative phase and modifies the ionospheric and thermospheric O/N2 local ratio. These observations provide insights into the complex interplay between solar events, geomagnetic activity, and ionospheric changes [12] [13].

4. Discussion

We presented a survey on the impact of solar activities on the ionospheric parameters *i.e.*, electron densities and critical frequency foF2 for three different stations of Japan *i.e.*, Okinawa, Kokubunji and Wakkanai on 23rd June 2015 as the maximum solar activities peaked at the solar cycle 24 was observed in the year 2015. From the resulting contour graphs (**Figures 3-5**), we observe a decrease in the electron densities on the day of the solar event. A noticeable trend was that as we moved higher with the latitude, the depletion was found to be more drastic. This is apparent in **Figure 5**. The Contour graph of Wakkanai shows that on the day of the event, *i.e.*, on 23 June, the value decreases to 2.740E + 11.

The two-step process of charge exchange followed by recombination contributes to O^+ chemical loss in the F-region of the ionosphere. Dissociative recombination is expedited with rising ion temperatures, enhancing O^+ recombination rates. This process involves NO^+ and O_2^+ recombining with electrons, forming neutral oxygen and nitrogen. Frictional heating draws neutral nitrogen and oxygen from lower altitudes into the F region. The resulting increased concentrations lead to enhanced recombination rates, causing a drop in electron density. High-latitude troughs, associated with frictional heating, occur when there's a notable difference in ion and neutral velocities, in contrast to mid-latitude troughs, typically resulting from extended recombination of ionospheric plasma.

As a significant layer of the atmosphere, the ionosphere possesses physical and chemical characteristics that are influenced by incident radiation and regional energetic processes. Particularly, the lower ionospheric region and the variations in its properties are crucial for human life and a variety of Earthly activities, necessitating continual measurements, observations, and the use of available data. Geomagnetic storms are linked to both the suppression and amplification of abnormalities. At low and middle latitudes, extreme events may result in over-shielding, PPEF, and fluctuating electric fields, especially if magnetospheric ring current plasma is augmented in a way that encourages such effects.

As a consequence, the ionospheric phenomenon becomes notably complex during strong to severe geomagnetic disturbances. The complexity is heightened over anomaly crest stations, presenting challenges in explanation through storm-induced disturbances alone. Factors like Prompt Penetration of high latitudinal electric field, heating by particle precipitation, disturbances in Dynamo Electric field (DDE), injection of charged particles, and the generation and penetration of high-energetic charge contribute to the intricate nature of the atmospheric system during magnetic storms. This multifaceted interplay underscores the need for a comprehensive understanding of various influences on ionospheric behavior during such events.

5. Conclusion

The obtained results highlight a strong correlation between ionospheric foF2 and electron density during perturbed geomagnetic conditions, revealing a decrease in both parameters during the geomagnetic storm event. An intriguing finding is a positive enhancement of 20% in the critical frequency foF2 over Wakkanai station at mid-latitudes, mostly observed on the day before the event, without apparent dependence on the time of day. Notably, variations in electron density and foF2 exhibit different patterns at various stations, even those in close proximity. This suggests that, during a specific period, factors or parameters undergo changes at different stations based on their latitude.

Conflicts of Interest

The authors have no conflict of interest.

References

[1] Balan, N. and Iyer, K.N. (1983) Equatorial Anomaly in Ionospheric Electron Content and Its Relation to Dynamo Currents. *Journal of Geophysical Research*: *Space Physics*, **88**, 10259-10262. https://doi.org/10.1029/ja088ia12p10259

[2] Carlson, H.C. (1996) Incoherent Scatter Radar Mapping of Polar Electrodynamics. *Journal of Atmospheric and Terrestrial Physics*, **58**, 37-56. https://doi.org/10.1016/0021-9169(95)00018-6

[3] Breed, A.M., Goodwin, G.L. and Silby, J.H. (1998) Total Electron Content Measurements in the Southern Hemisphere Using GPS Satellites, 1991 to 1995. *Radio Science*, **33**, 1705-1726. https://doi.org/10.1029/98rs01856

[4] Huang, X. and Reinisch, B.W. (2001) Vertical Electron Content from Ionograms in Real Time. *Radio Science*, **36**, 335-342. https://doi.org/10.1029/1999rs002409

[5] Reinisch, B.W., Huang, X., Song, P., Sales, G.S., Fung, S.F., Green, J.L., *et al*. (2001) Plasma Density Distribution along the Magnetospheric Field: RPI Observations from Image. *Geophysical Research Letters*, **28**, 4521-4524. https://doi.org/10.1029/2001gl013684

[6] Sethi, N.K., Dabas, R.S. and Sharma, K. (2008) Comparison between IRI Predictions and Digital Ionosonde Measurements of hmF2 at New Delhi during Low and Moderate Solar Activity. *Journal of Atmospheric and Solar-Terrestrial Physics*, **70**, 756-763. https://doi.org/10.1016/j.jastp.2007.10.009

[7] Liu, J.Y. (1996) A Study of Quasi-16-Day Ionospheric Oscillations. *Radiophysics and Quantum Electronics*, **39**, 155-165. https://doi.org/10.1007/bf02275370

[8] Rama Rao, P.V.S., Gopi Krishna, S., Niranjan, K. and Prasad, D.S.V.V.D. (2006) Temporal and Spatial Variations in TEC Using Simultaneous Measurements from the Indian GPS Network of Receivers during the Low Solar Activity Period of 2004-2005. *Annales Geophysicae*, **24**, 3279-3292. https://doi.org/10.5194/angeo-24-3279-2006

[9] Liu, L., Wan, W., Ning, B., Pirog, O.M. and Kurkin, V.I. (2006) Solar Activity Variations of the Ionospheric Peak Electron Density. *Journal of Geophysical Research: Space Physics*, **111**, A08304. https://doi.org/10.1029/2006ja011598

[10] Buresova, D. and Lastovicka, J. (2001) Changes in the F1 Region Electron Density during Geomagnetic Storms at Low Solar Activity. *Journal of Atmospheric and Solar-Terrestrial Physics*, **63**, 537-544. https://doi.org/10.1016/s1364-6826(00)00167-x

[11] Liu, L., Wan, W. and Ning, B. (2004) Statistical Modeling of Ionospheric FoF2 over Wuhan. *Radio Science*, **39**, RS2013. https://doi.org/10.1029/2003rs003005

[12] Fang, T. and Forbes, J.M. (2012) Ionosphere Response to Recurrent Geomagnetic

Activity in 1974. *Journal of Geophysical Research: Space Physics*, **117**, A01318. https://doi.org/10.1029/2011ja017017

[13] Yao, Y., Liu, L., Kong, J. and Zhai, C. (2016) Analysis of the Global Ionospheric Disturbances of the March 2015 Great Storm. *Journal of Geophysical Research: Space Physics*, **121**, 12, 157-12, 170. https://doi.org/10.1002/2016ja023352